DNA synthesis, immunity, and a wide array of cellular processes (Choi and Koh, 1998). The physiologic significance of neuronal zinc release within the central nervous system is not clear, and its role in ischemic brain injury is controversial. After brain ischemia, there is a depletion of presynaptic bouton zinc and a concurrent accumulation of zinc in the cell bodies of vulnerable neurons (Koh *et al*, 1996). In addition, Sorensen *et al* (1998) found evidence for early Zn^{2+} translocation from presynaptic terminals into postsynaptic neuronal cell bodies in the rat cortex subjected to focal ischemia. It has been proposed that synaptic zinc or extracellular zinc acts as 'the cell-death ion' during neuronal damage, both *in vitro* and *in vivo* (Choi *et al*, 1998; Shabanzadeh *et al*, 2004; Koh *et al*, 1996; Canzoniero *et al*, 1999). Although some authors believe that zinc may have a protective function (Bancila *et al*, 2004; Matsushita *et al*, 1996), it has been shown that when the influx of chelatable extracellular Zn^{2+} into postsynaptic neurons is blocked by intraventricular injection of a Zn^{2+}-chelating agent, neurodegeneration is prevented (Calderone *et al*, 2004). However, measurements of the change in intracerebral zinc concentrations are lacking after intravenous administration of EDTA at the time of cerebral ischemia. We therefore administered propofol EDTA (including 0.005% EDTA) intravenously, and measured zinc concentrations with or without cerebral ischemia. When propofol EDTA was administered without ischemia, no change was found in the intracerebral concentrations of zinc. However, the zinc concentration decreased significantly in the cortex, but not in the subcortex, when propofol EDTA was administered 10 mins before MCAO (Table 2). This result indicates that chelation of zinc by EDTA occurs in the cortex during ischemia, possibly resulting in a neuroprotective effect. However, further experiments will be needed to clarify the detailed mechanisms linking zinc to ischemic neuronal damage. Sorensen *et al* (1998) found that the density of zinc-positive terminals was significantly decreased in the neocortical ischemic zone at 7 mins after MCAO in rats. In addition, Foreman *et al* (1953) injected $CaNa_2EDTA$ into a rat muscle, and found that the metabolic turnover time was approximately 50 mins. On the basis of these findings, we decided to sample brain at 1 h after MCAO. However, we did not try to determine when the level of zinc accumulation in the extracellular space or postsynaptic neuron reaches a peak or when the chelated zinc begins to be egested from the brain.

Second, we did not assess the proportion of zinc chelated by propofol EDTA. Although some investigations have found that Zn^{2+} chelators protect against ischemic cell death, there is a view that 'too much extracellular Zn^{2+} has toxic effects, but some concentrations of Zn^{2+} have neuroprotective effects' (Zhao *et al*, 1996; Kitamura *et al*, 2006). We therefore need to study the relationship between the proportion of chelated zinc and the associated neuroprotective effects.

Lastly, EDTA can also chelate calcium. An intracellular calcium increase is an early key event triggering ischemic neuronal cell damage (Nikonenko *et al*, 2005). There is therefore a possibility that EDTA protects cells by modulating calcium influx into the cells, and it is consequently impossible to ascribe the neuroprotective effects of EDTA to a chelation of zinc alone (since we did not measure the concentration of calcium).

In this study, we found that pretreatment with EDTA robustly protects neurons. In principle, chelation therapy using EDTA could be a new treatment for cerebral ischemia. In fact, chelation therapy using intravenous injections of edetate disodium was being promoted to the public two decades ago as a nonsurgical means of treating coronary or other arterial atherosclerosis (Rathmann and Golightly, 1984). However, subsequent researchers have provided no evidence that chelation therapy is efficacious beyond a powerful placebo effect (Ernst, 1997; Shrihari *et al*, 2006). Moreover, the loss of essential minerals and the possible redistribution of lead within the body may constitute disadvantages that should be taken into account if contemplating repeated intravenous administration of EDTA. Herr *et al* (2000) compared the safety of propofol with that of propofol EDTA when used for sedation in critically ill postsurgical or trauma patients in the intensive care unit. The propofol EDTA formulation had no effects on calcium or magnesium homeostasis, renal function, or sedation efficacy over and above of propofol alone when used for sedation in critically ill surgical or intensive care

Table 2 Zinc levels in mouse brains

Treatments	*Ischemia*	*Cortex (μg/g)*	*% of vehicle*	*Subcortex (μg/g)*	*% of vehicle*
Vehicle	−	139.9±42.6	100	110.3±30.1	100
Propofol EDTA	−	137.0±32.0	97.9	108.0±36.5	97.9
Vehicle	+	150.2±36.7	107.4	107.3±30.4	97.3
Propofol EDTA	+	120.8±22.4*	86.3	98.6±19.2	89.4

*$P < 0.05$ versus vehicle (+ ischemia) group (Bonferroni correction).
Propofol EDTA (10 mg/kg intravenously) or vehicle (intralipid) was administered at 10 mins before ischemia. Mice were killed 1 h after the onset of ischemia. Nonischemic groups were killed 1 h after drug (or vehicle) administration. Values are mean±s.d. ($n = 10$).

unit patients. In addition, Zaloga and Teres (2000) reported that the most notable abnormality in intensive care unit patients given propofol containing EDTA was a low blood zinc level, but no adverse events indicative of zinc deficiency occurred. Such a decrease in the blood zinc concentration by EDTA accords with our result (decrease in the concentration of zinc in brain tissue). However, since EDTA-induced chelation of calcium has the capacity to kill cells, we believe that it is also necessary to consider its concentration when EDTA is administered intravenously.

In summary, propofol and EDTA each inhibited OGD-induced cell damage, cotreatment with propofol and EDTA being more potent than treatment with propofol alone. Propofol EDTA decreased ischemic neuronal damage after MCAO in mice, and its potency was greater than that of propofol alone. These findings indicate that EDTA may itself have a neuroprotective effect, perhaps partially due to its chelation of zinc.

References

Adembri C, Venturi L, Tani A, Chiarugi A, Gramigni E, Cozzi A, Pancani T, De Gaudio RA, Pellegrini-Giampietro DE (2006) Neuroprotective effects of propofol in models of cerebral ischemia: inhibition of mitochondrial swelling as a possible mechanism. *Anesthesiology* 104: 80–9

Bancila V, Nikonenko I, Dunant Y, Bloc A (2004) Zinc inhibits glutamate release via activation of pre-synaptic K channels and reduces ischaemic damage in rat hippocampus. *J Neurochem* 90:1243–50

Brown ET, Umino Y, Loi T, Solessio E, Barlow R (2005) Anesthesia can cause sustained hyperglycemia in C57/BL6J mice. *Vis Neurosci* 22:615–8

Calderone A, Jover T, Mashiko T, Noh KM, Tanaka H, Bennett MV, Zukin RS (2004) Late calcium EDTA rescues hippocampal CA1 neurons from global ischemia-induced death. *J Neurosci* 24:9903–13

Canzoniero LM, Turetsky DM, Choi DW (1999) Measurement of intracellular free zinc concentrations accompanying zinc-induced neuronal death. *J Neurosci* 19:RC31

Choi DW, Koh JY (1998) Zinc and brain injury. *Annu Rev Neurosci* 21:347–75

Choi DW, Yokoyama M, Koh J (1998) Zinc neurotoxicity in cortical cell culture. *Neuroscience* 24:67–79

Ernst E (1997) Chelation therapy for peripheral arterial occlusive disease: a systematic review. *Circulation* 96:1031–3

Fenstermacher J, Kaye T (1998) Drug 'diffusion' within the brain. *Ann NY Acad Sci* 531:29–39

Foreman H, Vier M, Magee M (1953) The metabolism of C14 labeled ethylenediaminetetraacetic acid in the rat. *J Biol Chem* 203:1045–53

Hara H, Friedlander RM, Gagliardini V, Ayata C, Fink K, Huang Z, Shimizu-Sasamata M, Yuan J, Moskowitz MA (1997) Inhibition of interleukin 1β converting enzyme family proteases reduces ischemic and excitotoxic neuronal damage. *Proc Natl Acad Sci USA* 94:2007–12

Hara H, Huang PL, Panahian N, Fishman MC, Moskowitz MA (1996) Reduced brain edema and infarction volume in mice lacking the neuronal isoform of nitric oxide synthase after transient MCA occlusion. *J Cereb Blood Flow Metab* 16:605–11

Herr DL, Kelly K, Hall JB, Ulatowski J, Fulda GJ, Cason B, Hickey R, Nejman AM, Zaloga GP, Teres D (2000) Safety and efficacy of propofol with EDTA when used for sedation of surgical intensive care unit patients. *Intensive Care Med* 26:S452–62

Ito H, Watanabe Y, Isshiki A, Uchino H (1999) Neuroprotective properties of propofol and midazolam, but not pentobarbital, on neuronal damage induced by forebrain ischemia, based on the GABAA receptors. *Acta Anaesthesiol Scand* 43:153–62

Kitagawa H, Hayashi T, Mitsumoto Y, Koga N, Itoyama Y, Abe K (1998) Reduction of ischemic brain injury by topical application of glial cell line-derived neurotrophic factor after permanent middle cerebral artery occlusion in rats. *Stroke* 29:1417–22

Kitamura Y, Iida Y, Abe J, Ueda M, Mifune M, Kasuya F, Ohta M, Igarashi K, Saito Y, Saji H (2006) Protective effect of zinc against ischemic neuronal injury in a middle cerebral artery occlusion model. *J Pharmacol Sci* 100:142–8

Koh JY, Suh SW, Gwag BJ, He YY, Hsu CY, Choi DW (1996) The role of zinc in selective neuronal death after transient global cerebral ischemia. *Science* 272: 1013–6

Marik PE (2004) Propofol: therapeutic indications and side-effects. *Curr Pharm Des* 10:3639–49

Matsushita K, Kitagawa K, Matsuyama T, Ohtsuki T, Taguchi A, Mandai K, Mabuchi T, Yagita Y, Yanagihara T, Matsumoto M (1996) Effect of systemic zinc administration on delayed neuronal death in the gerbil hippocampus. *Brain Res* 743:362–5

Miyawaki T, Yokota H, Oguro K, Kato K, Shimazaki K (2004) Ischemic preconditioning decreases intracellular zinc accumulation induced by oxygen–glucose deprivation in gerbil hippocampal CA1 neurons. *Neurosci Lett* 362:216–9

Nikonenko I, Bancila M, Bloc A, Muller D, Bijlenga P (2005) Inhibition of T-type calcium channels protects neurons from delayed ischemia-induced damage. *Mol Pharmacol* 68:84–9

Pittman JE, Sheng H, Pearlstein R, Brinkhous A, Dexter F, Warner DS (1997) Comparison of the effects of propofol and pentobarbital on neurologic outcome and cerebral infarct size after temporary focal ischemia in the rat. *Anesthesiology* 87:1139–44

Rathmann KL, Golightly LK (1984) Chelation therapy of atherosclerosis. *Drug Intell Clin Pharm* 18:1000–3

Sagara Y, Hendler S, Khoh-Reiter S, Gillenwater G, Carlo D, Schubert D, Chang J (1999) Propofol hemisuccinate protects neuronal cells from oxidative injury. *J Neurochem* 73:2524–30

Shabanzadeh AP, Shuaib A, Yang T, Salam A, Wang CX (2004) Effect of zinc in ischemic brain injury in an embolic model of stroke in rats. *Neurosci Lett* 356: 69–71

Shrihari JS, Roy A, Prabhakaran D, Reddy KS (2006) Role of EDTA chelation therapy in cardiovascular diseases. *Natl Med J India* 19:24–6

Sitar SM, Hanifi-Moghaddam P, Gelb A, Cechetto DF, Siushansian R, Wilson JX (1999) Propofol prevents peroxide-induced inhibition of glutamate transport in cultured astrocytes. *Anesthesiology* 90:1446–53

Sorensen JC, Mattsson B, Andreasen A, Johansson BB (1998) Rapid disappearance of zinc positive terminals in focal brain ischemia. *Brain Res* 812:265–9

Tsai YC, Huang SJ, Lai YY, Chang CL, Cheng JT (1994) Propofol does not reduce infarct volume in rats undergoing permanent middle cerebral artery occlusion. *Acta Anaesthesiol Sin* 32:99–104

Wilson JX, Gelb AW (2002) Free radicals, antioxidants, and neurologic injury: possible relationship to cerebral protection by anesthetics. *J Neurosurg Anesthesiol* 14:66–79

Young Y, Menon DK, Tisavipat N, Matta BF, Jones JG (1997) Propofol neuroprotection in a rat model of ischaemia reperfusion injury. *Eur J Anaesthesiol* 14:320–6

Zaloga GP, Teres D (2000) The safety and efficacy of propofol containing EDTA: a randomised clinical trial programme focusing on cation and trace metal homeostasis in critically ill patients. *Intensive Care Med* 26:S398–9

Zhan RZ, Qi S, Wu C, Fujihara H, Taga K, Shimoji K (2001) Intravenous anesthetics differentially reduce neurotransmission damage caused by oxygen–glucose deprivation in rat hippocampal slices in correlation with *N*-methyl-D-aspartate receptor inhibition. *Crit Care Med* 29:808–13

Zhao YJ, Yang GY, Domino EF (1996) Zinc protoporphyrin, zinc ion, and protoporphyrin reduce focal cerebral ischemia. *Stroke* 27:2299–303

BRAIN RESEARCH 1214 (2008) 169–176

available at www.sciencedirect.com

ScienceDirect

www.elsevier.com/locate/brainres

BRAIN RESEARCH

Research Report

Protective effects of SUN N8075, a novel agent with antioxidant properties, in *in vitro* and *in vivo* models of Parkinson's disease

A. Oyagi[a], Y. Oida[a], H. Hara[b], H. Izuta[a], M. Shimazawa[a], N. Matsunaga[a], T. Adachi[b], H. Hara[a,*]

[a]Department of Biofunctional Evaluation, Molecular Pharmacology, Gifu Pharmaceutical University, 5-6-1 Mitahora-higashi, Gifu 502-8585, Japan

[b]Department of Biomedical Pharmaceutics, Clinical Pharmaceutics, Gifu Pharmaceutical University, 5-6-1 Mitahora-higashi, Gifu 502-8585, Japan

ARTICLE INFO

Article history:
Accepted 24 February 2008
Available online 6 March 2008

Keywords:
Antioxidant
MPTP
6-OHDA
Parkinson disease
SUN N8075

ABSTRACT

SUN N8075 is a novel antioxidant with neuroprotective properties. This study was designed to elucidate its neuroprotective effects against 6-hydroxy dopamine (6-OHDA)-induced cell death and 1-methyl-4-phenyl-1,2,3,6-tetrahydropyridine (MPTP)-induced neurotoxicity (known as *in vitro* and *in vivo* models of Parkinson's disease, respectively). In the *in vitro* study, on human neuroblastoma SH-SY5Y cells, SUN N8075 decreased the hydrogen peroxide (H_2O_2)-induced production of reactive oxygen species and protected against 6-OHDA-induced cell death. In the *in vivo* study, SUN N8075, when injected intraperitoneally (i.p.) twice with a 5-h interval, inhibited lipid peroxidation (viz. the production of thiobarbituric acid reactive substance) in the mouse forebrain at 1 h after the second injection. Mice were injected i.p. with MPTP (10 mg/kg) four times at 1-h intervals, and brains were analyzed 7 days later. SUN N8075 at 30 mg/kg (i.p., twice) exhibited a protective effect against the MPTP-induced decrease in tyrosine hydroxylase (TH)-positive fibers in the striatum. Moreover, SUN N8075 at 10 and 30 mg/kg (i.p., twice) had a similar protective effect against the MPTP-induced decrease in TH-positive cells in the substantia nigra. Further, SUN N8075 30 mg/kg (i.p. twice) markedly suppressed the MPTP-induced accumulation of 8-hydroxy-deoxyguanosine (8-OHdG) in the striatum. These findings indicate that SUN N8075 exerts protective effects, at least in part via an anti-oxidation mechanism, in these *in vitro* and *in vivo* models of Parkinson's disease.

1. Introduction

Parkinson's disease is characterized by the progressive and selective loss of dopaminergic neurons that project from the substantia nigra pars compacta to the striatum. Although the pathogenesis of Parkinsonism remains obscure, exposure of such dopaminergic neurons in the substantia nigra pars compacta to oxidative stress is believed to be one of the leading causes of neurodegeneration in Parkinson's disease. Antioxidants, as scavengers of reactive oxygen species (ROS) and free radicals, may play an important role in the prevention of Parkinson's disease (Grimes et al., 1988).

Hydroxydopamine (6-OHDA), an oxidative neurotoxin, has been used to lesion the nigrostriatal system that degenerates

* *Corresponding author.* Fax: +81 58 237 8596.
E-mail address: hidehara@gifu-pu.ac.jp (H. Hara).

0006-8993/$ – see front matter © 2008 Elsevier B.V. All rights reserved.
doi:10.1016/j.brainres.2008.02.073

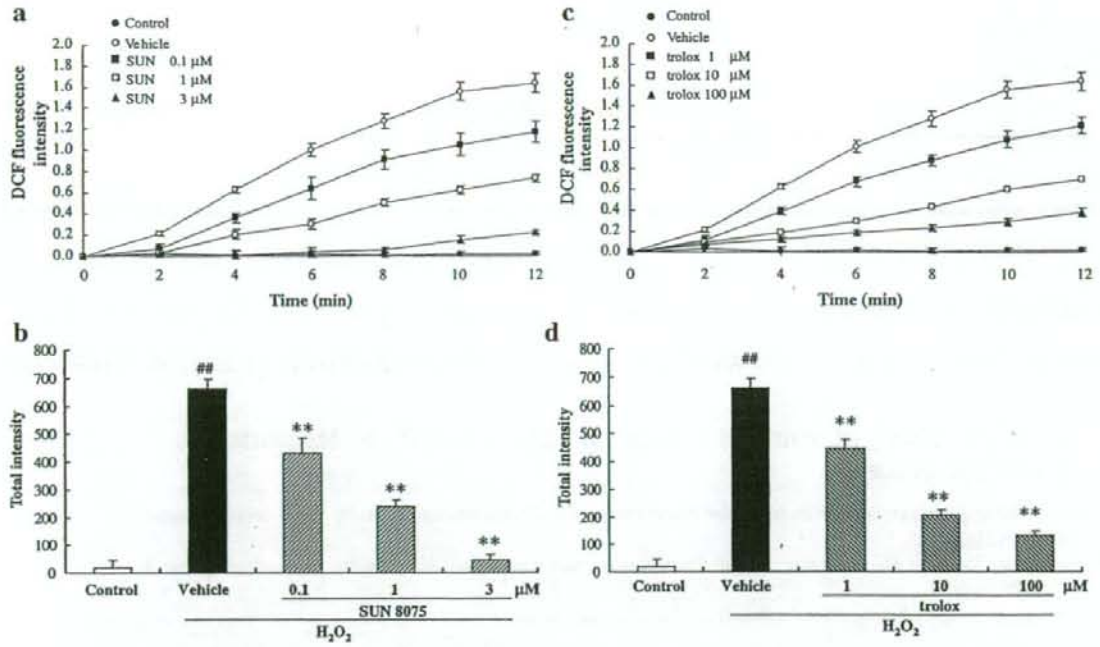

Fig. 1 – Effects of SUN N8075 and trolox on hydrogen peroxide (H_2O_2)-induced production of reactive oxygen species (ROS). Measurement of ROS induced by H_2O_2. (a) SH-SY5Y cells were exposed to H_2O_2 at 300 μM in the presence of SUN N8075 at 0.1 μM (■), 1.0 μM (□), or 10 μM (▲). Control group (•), vehicle group (○). Immediately thereafter, the intracellular ROS levels were determined by measuring the fluorescence of H_2DCF-DA every 2 min. (b) Total intensity was calculated from (a), as described in "Experimental procedures". (c) SH-SY5Y cells were exposed to H_2O_2 at 300 μM in the presence of trolox at 1 μM (■), 10 μM (□), or 100 μM (▲). Control group (•), vehicle group (○). (d) Total intensity was calculated from (c). Values are expressed as the mean ± S.E. ##P<0.01 vs. Control, **P<0.01 vs. Vehicle (n=4).

in Parkinson's and related diseases, to ablate the sympathetic nervous system, and as a chemotherapeutic agent for catecholaminergic neoplasms (Przedborski and Ischiropoulos, 2005; Schneider and Markham, 1986). In humans and rodents, 1-methyl-4-phenyl-1,2,3,6-tetrahydropyridine (MPTP) is also well-known to produce clinical, biochemical, and neurochemical changes similar to those that occur in Parkinson's disease (Heikkila et al., 1984; Turski et al., 1991). This neurotoxin also

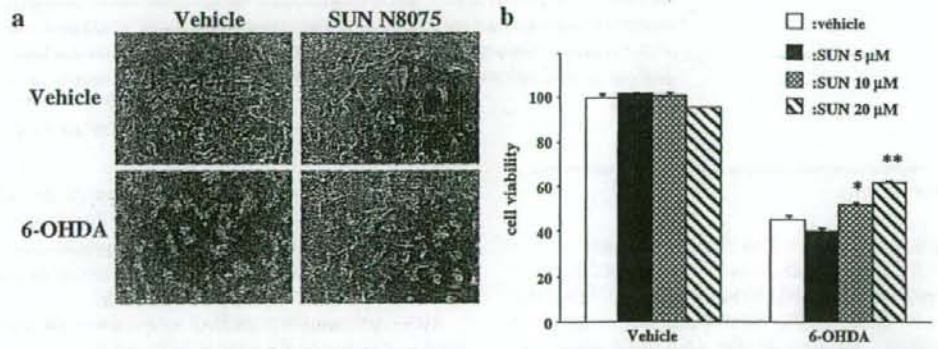

Fig. 2 – Effect of SUN N8075 on 6-OHDA-induced cell death in SH-SY5Y cells. (a) Morphological changes in SH-SY5Y cells. Scale bar=50 μm. (b) SH-SY5Y cells were exposed to 6-OHDA (50 μM) in the presence of SUN N8075 (5, 10, or 20 μM). Eighteen hours later, cell viability was measured using an MTT assay. Results are expressed as percentages, relative to cells treated with vehicle alone. Values (means ± S.E.) were derived from four separate cultures. *P<0.05, **P<0.01 vs. cells treated with 6-OHDA alone (n=4). SUN: SUN N8075.

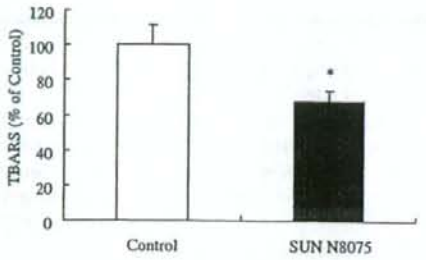

Fig. 3 – Effect of SUN N8075 on lipid peroxidation in mouse brain homogenates. Mouse brain homogenates, from mice intraperitoneally injected twice either with SUN N8075 30 mg/kg or with saline, were incubated at 37 °C for 30 min. Absorbance of thiobarbituric acid reactive substance (TBARS) was measured. Values are expressed as the mean ± S.E. *P<0.05 vs. Control (n=10).

causes both a marked depletion of the striatal dopamine content and decreases in the number of nigrostriatal dopaminergic neurons in several species, including monkeys, dogs, cats, and mice (Burns et al., 1983; Hantraye et al., 1996; Johannessen et al., 1991; Ricaurte et al., 1986; Schneider and Markham, 1986). Hence, 6-OHDA and MPTP are commonly used to generate experimental models of Parkinson's disease in both *in vitro* and *in vivo* studies.

SUN N8075, (2S)-1-(4-amino-2,3,5-trimethylphenoxy)-3-[4-[4-(4-fluorobenzyl)phenyl]-1-piperazinyl]-2-propanol dimethanesulfonate, is a novel antioxidant that is currently in clinical trials for stroke (Annoura et al., 2000). Its anti-oxidative effects contribute to a diminution of the damage induced by ROS during cerebral ischemia and reperfusion (Robins, 2004). Our previous study revealed a potent neuroprotective activity of this agent in an *in vivo* transient middle cerebral artery occlusion model, suggesting that the underlying neuroprotective mechanism may partly involve protection against oxidative stress (Kotani et al., 2007). However, the neuroprotective effects of SUN N8075 have not been studied in animal models of Parkinson's disease.

Therefore, in the present study, we (a) investigated its effects *in vitro* on both H_2O_2-induced ROS production and 6-OHDA-induced cell death, using human neuroblastoma SH-SY5Y cells, and (b) evaluated its putative neuroprotective effects on MPTP-induced neurotoxicity in an *in vivo* mouse model of Parkinson's disease.

2. Results

2.1. *Effects of SUN N8075 on hydrogen peroxide (H_2O_2)-induced reactive oxygen species (ROS)*

First, we investigated the effects of SUN N8075 on the H_2O_2-induced production of ROS in SH-SY5Y cells. Treatment with H_2O_2 increased ROS in a time-dependent manner, and this

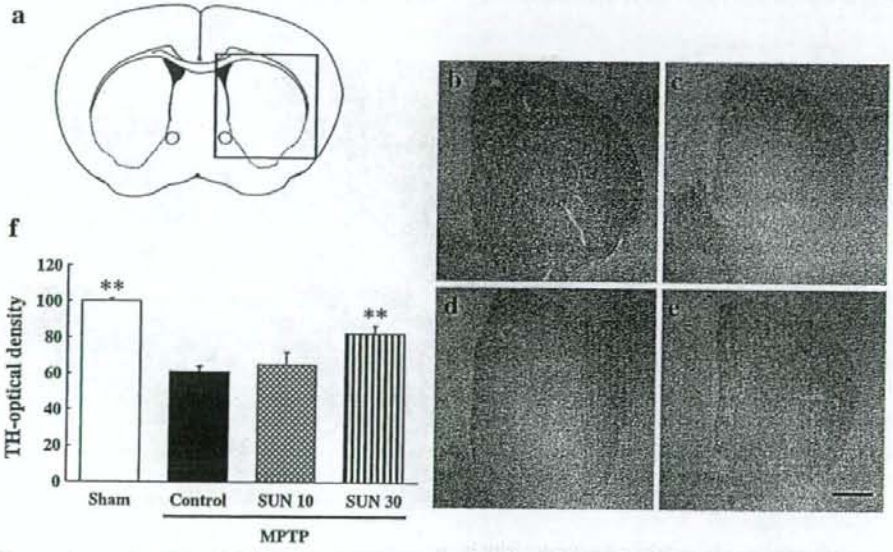

Fig. 4 – Effect of SUN N8075 on MPTP-induced neurotoxicity in the striatum of mice. SUN N8075 attenuated the immunohistochemical changes in tyrosine hydroxylase (TH) induced by 1-methyl-4-phenyl-1,2,3,6-tetrahydropyridine (MPTP) in mouse striatum. (a) Coronal section through the striatum; square, area shown in the microphotographs. (b) Sham group (Sham). (c) Seven days after MPTP + vehicle treatment (Control). (d) Seven days after MPTP + SUN N8075 (10 mg/kg i.p., twice) treatment (SUN 10). (e) Seven days after MPTP + SUN N8075 (30 mg/kg i.p., twice) treatment (SUN 30). (f) Optical density of TH-positive fibers in striatum. A decrease in the number of TH-immunopositive fibers was observed in the striatum at 7 days after MPTP treatment (c,f). SUN N8075 (30 mg/kg i.p., twice) partly prevented this decrease (e,f). Scale bar = 150 μm. Values are expressed as the mean ± S.E. **P<0.01 vs. Control (n=8 or 9).

ROS production was decreased by SUN N8075 and also by a water-soluble vitamin E analogue (trolox) (Fig. 1a,c). When ROS production was expressed as "Total intensity", pretreatment with SUN N8075 at 0.1 to 3 μM or with trolox at 1 to 100 μM concentration-dependently and significantly reduced it, and the IC_{50} values being 0.32 μM (95% confidence limits, 0.16–0.52) and 4.6 μM (2.69–7.26), respectively (Fig. 1b,d).

2.2. *Effect of SUN N8075 on 6-OHDA-induced cell death*

Next, to elucidate the effects of SUN N8075 on 6-OHDA-induced neurotoxicity *in vitro*, SH-SY5Y cells were exposed to 6-OHDA at 50 μM in the presence or absence of SUN N8075. As shown in Fig. 2, SUN N8075 protected against 6-OHDA-induced cell death in a dose-dependent manner.

2.3. *Effects of SUN N8075 on lipid peroxidation in mouse brain homogenate*

In this experiment, SUN N8075 (at 30 mg/kg) or saline was administered intraperitoneally twice, and at 1 h after the second administration, the brains were removed. After a 30-min incubation at 37 °C, the thiobarbituric acid reactive substance (TBARS) level in the brain homogenates was increased. SUN N8075 (at 30 mg/kg i.p., twice) significantly inhibited this production of TBARS by about 30% versus vehicle treatment (Fig. 3).

2.4. *Body weight change after MPTP administration*

We evaluated the effect of SUN N8075 using an MPTP-induced neurotoxic model *in vivo*. At 1 day after MPTP administration, the body weight of mice in the control (vehicle+MPTP administration) group had decreased by approximately 10% (versus before administration), but it had gradually returned to normal at 3 days after MPTP administration (before administration: 24.5±0.3 g, 1 day after administration: 23.6±0.4 g, 3 days after administration: 24.3±0.6 g). The body weights of mice treated with SUN N8075 showed no significant differences from those of the control group: SUN N8075 10 mg/kg: 23.1±0.5 g, 22.4±0.4 g, 23.6±0.4 g, SUN N8075 30 mg/kg: 24.4±0.3 g, 23.9±0.3 g, 24.8±0.2 g, respectively.

2.5. *Effects of SUN N8075 on MPTP-induced decrease in tyrosine hydroxylase (TH)-positive density in the striatum*

Representative photomicrographs of TH immunostaining in the striatum are shown in Fig. 4b–e. Striatal fibers displayed strong TH-immunostaining in Sham mice (Fig. 4b). A decrease in the density of TH-immunopositive fibers was observed at 7 days after MPTP administration (Fig. 4c,f). SUN N8075 at 30 mg/kg significantly reduced this effect of MPTP (Fig. 4e,f).

2.6. *Effect of SUN N8075 on MPTP-induced decrease in tyrosine hydroxylase (TH)-positive cells in the substantia nigra*

Representative photomicrographs of TH immunostaining in the substantia nigra are shown in Fig. 5b–e. Nigral TH-immunoreactive neurons were easily detectable in Sham mice (Fig. 5b). A decrease in the number of TH-immunopositive neurons was observed at 7 days after MPTP administration (Fig. 5c,f). SUN N8075 at 10 and 30 mg/kg significantly reduced this effect of MPTP (Fig. 5d,e,f).

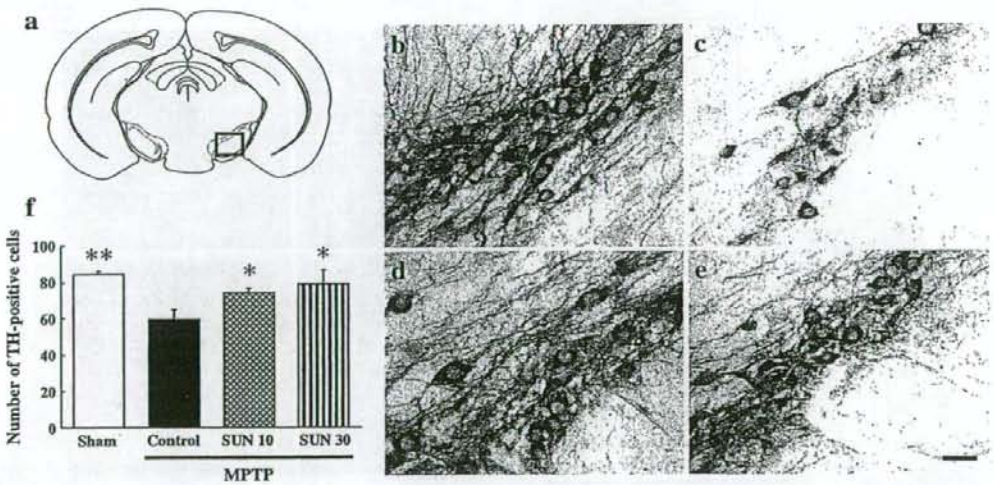

Fig. 5 – Effect of SUN N8075 on MPTP-induced neurotoxicity in the substantia nigra of mice. SUN N8075 attenuated the immunohistochemical changes in tyrosine hydroxylase (TH) induced by 1-methyl-4-phenyl-1,2,3,6-tetrahydropyridine (MPTP) in mouse substantia nigra. (a) Coronal section through the substantia nigra; square, area shown in the microphotographs. (b) Sham group (Sham). (c) Seven days after MPTP+vehicle treatment (Control). (d) Seven days after MPTP+SUN N8075 (10 mg/kg i.p., twice) treatment (SUN 10). (e) Seven days after MPTP+SUN N8075 (30 mg/kg i.p., twice) treatment (SUN 30). (f) Number of TH-positive cells in substantia nigra. A decrease in the number of TH-immunopositive neurons in the substantia nigra was observed at 7 days after MPTP treatment (c,f). SUN N8075 (10 and 30 mg/kg i.p., twice) partly prevented this decrease (d,e,f). Scale bar=30 μm. Values are expressed as the mean±S.E. *P<0.05, **P<0.01 vs. Control (n=8 or 9).

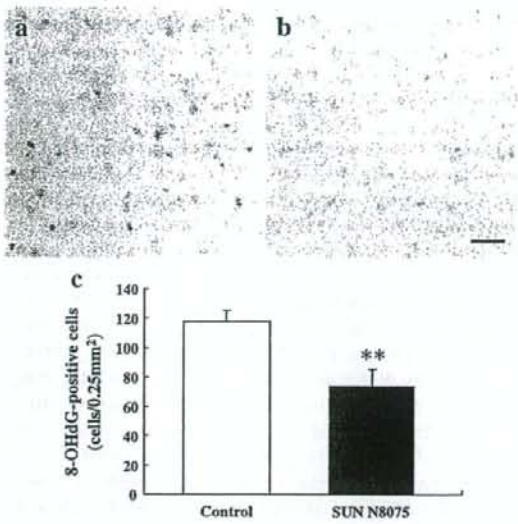

Fig. 6 – Effect of SUN N8075 on the expression of 8-OHdG induced by MPTP in the striatum of mice. Oxidative DNA damage was assessed by measuring 8-OHdG immunoreactivity. Shown are 8-OHdG-positive cells in the striatum at 7 days after MPTP + vehicle treatment (Control) (a), and MPTP + SUN N8075 (30 mg/kg i.p., twice) treatment (SUN 30) (b). (c) Numbers of 8-OHdG-positive cells in the striatum. Scale bar = 30 μm. Values are expressed as the mean ± S.E. **P < 0.01 vs. Control (n = 5 or 7).

2.7. *Anti-oxidative effect of SUN N8075 on MPTP-induced oxidative DNA damage*

We examine the neuroprotective effects of SUN N8075 against MPTP-induced oxidative stress by performing immunohistochemical analysis for 8-OHdG, a marker of DNA damage, in the striatum. No positive staining was detected in the sham-operation group (data not shown). Seven days after MPTP administration, strong 8-OHdG immunoreactivity was detected in the control group (Fig. 6a,c). SUN N8075 at 30 mg/kg significantly reduced the number of 8-OHdG-positive cells (Fig. 6b,c).

3. Discussion

In the present study, *in vitro* and *in vivo* models of Parkinson's disease were used to examine the neuroprotective properties of SUN N8075. We first evaluated its protective effect *in vitro* against 6-OHDA-induced cell death, a model of Parkinson's disease, using human neuroblastoma SH-SY5Y cells. When SH-SY5Y cells were exposed to 6-OHDA in the presence of SUN N8075, SUN N8075 reduced the 6-OHDA-induced cell death in a dose-dependent manner (Fig. 2). Although the precise mechanism underlying 6-OHDA-induced neurotoxicity remains unknown, it has been reported that 6-OHDA directly inhibits mitochondrial respiratory complexes I and IV, leading to depletion of ATP (Glinka et al., 1997). *In vitro* and *in vivo* experiments have revealed that antioxidants prevent the loss of dopaminergic neurons caused by 6-OHDA (Gassen et al., 1998; Hara et al., 2003; Soto-Otero et al., 2000). These findings suggest that ROS plays a critical role in 6-OHDA-induced neurotoxicity. After being selectively taken up via the dopamine transporter present in dopaminergic neurons, 6-OHDA is thought to be autooxidized, resulting in the generation of ROS. Interestingly, we also found that SUN N8075 reduced H_2O_2-induced ROS production in SH-SY5Y cells (Fig. 1), its inhibitory effect being more than 10 times stronger than that of the well-known antioxidant trolox (a water-soluble vitamin E analogue). These findings indicate that the neuroprotective effect of SUN N8075 against 6-OHDA-induced neurotoxicity may be due, at least in part, to a scavenging effect on ROS.

Next, we evaluated the effect of SUN N8075 against oxidative stress in an *in vivo* model. SUN N8075 (at 30 mg/kg, i.p., twice) exhibited a potent antioxidant action against lipid peroxidation in a mouse brain homogenate (Fig. 3), suggesting that this agent penetrates the blood-brain barrier and is distributed into the brain, there to exert an anti-oxidative effect. MPTP increases the lipid peroxidation product thiobarbituric acid reactive substance (TBARS), and major antioxidants reduce the TBARS level in the midbrain (Kawasaki et al., 2007; Sankar et al., 2007). In the present study, reductions in the levels of TH immunoreactivity were observed in both the striatum and substantia nigra at 7 days after MPTP administration, results that are consistent with those in previous reports (Araki et al., 2001; Watanabe et al., 2004). SUN N8075 exhibited protective effects against MPTP-induced neurotoxic damage in both the striatum (Fig. 4) and the substantia nigra (Fig. 5). The neurotoxic effects of MPTP is dependent on an inhibition of complex I in the mitochondrial respiratory chain by MPP^+, subsequently followed by ATP depletion and an increased production of ROS, leading eventually to cell death (Ali et al., 1994; Nicklas et al., 1985). In the present study, MPTP induced an accumulation of 8-OHdG, a marker of oxidative stress, and this accumulation was partially suppressed by SUN N8075 (Fig. 6). 8-OHdG is formed in a promutagenic DNA lesion induced by the reaction of hydroxyl radicals with guanosine at the C8 site in DNA (Kasai and Nishimura, 1986). The urinary 8-OHdG level increases with the stage of Parkinson's disease, and urinary 8-OHdG has been reported to be a potentially useful biomarker for evaluating the progression of Parkinson's disease (Sato et al., 2005). Taken together, the above suggests to us that inhibition of lipid peroxidation and 8-OHdG may be one of the mechanisms by which SUN N8075 exerts neuroprotection against MPTP-induced neurodegeneration.

The results we observed *in vitro* and *in vivo* indicate that the neuroprotective action of SUN N8075 may be mediated via an antioxidant effect. ROS scavenging is probably the mechanism by which SUN N8075 afforded neuroprotection in our *in vitro* study, while inhibitions of 8-OHdG accumulation and lipid peroxidation, both induced by oxidative stress, are the most likely mechanisms by which it afforded neuroprotection in our *in vivo* study. The current data conforms with previous reports showing that SUN N8075 is a novel antioxidant (Annoura et al., 2000) and has governed potent neuroprotective activity in an *in vivo* ischemia model (Kotani et al., 2007).

After subcutaneous injection of SUN N8075 (10–30 mg/kg), its concentration in plasma was approximately 1.5–3.0 μM (Tamura S. et al., unpublished data). As injected intraperitoneally in our

study, we can expect much higher plasma concentration than in the case of subcutaneous injection. Taken together, the concentration of SUN N8075 in plasma was almost consistent with its *in vitro* effect.

In conclusion, we found that SUN N8075 provided neuroprotection in both *in vitro* and *in vivo* models of Parkinson's disease. An inhibitory effect of SUN N8075 against oxidative stress may be partly responsible for these observed neuroprotective effects. These findings indicate that SUN N8075 has the potential to be used to retard or prevent the progression of Parkinson's disease.

4. Experimental procedures

4.1. Animals

Male C57BL/6 mice (Nihon SLC, Shizuoka, Japan), weighing 22–28 g, were used for experiments involving MPTP administration. All animals were allowed food and water ad libitum, and they were housed in a temperature-controlled environment (22±2 °C) under a 12-h light/dark cycle. The experiments were conducted in accordance with the Animal Care Guidelines issued by the Animal Experimental Committee of Gifu Pharmaceutical University.

4.2. Experimental materials

The drugs used and their sources were as follows. SUN N8075, (2S)-1-(4-amino-2,3,5-trimethylphenoxy)-3-[4-[4-(4-fluorobenzyl)phenyl]-1-piperazinyl]-2-propanol dimethanesulfonate (Asubio Pharma, Tokyo, Japan), 1-methyl-4-phenyl-1,2,3,6-tetrahydropyridine (MPTP) hydrochloride (Sigma-Aldrich Co, St. Louis, USA), nembutal (Dainippon Pharmaceutical, Osaka, Japan), Vectastain elite ABC kit (Vector Labs, Burlingame, CA, USA), rabbit anti-TH polyclonal antibody (Chemicon, Temecula, CA, USA), mouse anti-8-OHdG hydrogen peroxidase (Wako Pure Chemical Industries, Osaka, Japan), methanol (Wako), paraformaldehyde (Wako), Dulbecco's modified Eagle's medium (DMEM; Sigma-Aldrich), fetal bovine serum (Valeant, CA, USA), penicillin and streptomycin (Meiji Seika, Tokyo, Japan), trolox (Sigma), $HClO_4$ (Sigma), thiobarbituric acid (Sigma). SUN N8075 (10 mg/kg and 30 mg/kg) and MPTP (10 mg/kg) were dissolved in saline before use and then intraperitoneally administered (0.1 ml/10 g).

4.3. Reactive oxygen species assay

The intracellular accumulation of ROS within SH-SY5Y cells was determined using Reactive Oxygen Species Detection reagents (Invitrogen, CA, USA). SUN N8075 at 0.1 to 3 μM or trolox at 1 to 100 μM was pre-treated for 1 h, and cells were then treated with H_2DCF-DA at 10 μM for 15 min. Thereafter, the whole medium was replaced with fresh medium containing the same compounds. After treatment with hydrogen peroxide (H_2O_2) at 300 μM, the increase in ROS levels was assessed by measuring the fluorescence of H_2DCF-DA (492 nm/525 nm: excitation/emission) using Varioskan Flash TOP/BOTTOM (Thermo, Kanagawa, Japan). "Total intensity" was calculated by integrating the area under the H_2DCF-DA fluorescence intensity curve for 12 min after H_2O_2 treatment. Results represent the average±S.E. of 4 independent experiments, with each treatment performed in duplicate.

4.4. 6-OHDA model in SH-SY5Y cells

Human neuroblastoma (SH-SY5Y) cells were cultured in DMEM supplemented with 10% fetal calf serum, 100 U/ml penicillin G, and 0.1 mg/ml streptomycin in a humidified 5% CO_2/95% air incubator at 37 °C. SH-SY5Y cells were seeded in a 96-well plate at a density of 1.5×10^4 cells. The next day, the culture medium was replaced with fresh medium, and cells were then treated for 18 h with 6-hydroxydopamine (6-OHDA; 50 μM) in the presence or absence of SUN N8075 (5, 10, or 20 μM). Cell viability was measured using a 3-(4,5-dimethylthiazol-2-yl)-2,5-diphenyl tetrazolium bromide (MTT) assay, the medium being replaced with fresh medium containing MTT (final concentration 0.5 mg/ml) followed by incubation for 2 h at 37 °C. Isopropanol with 0.04 N HCl was then added, and finally the optical density was measured at 570 nm by means of a microplate reader. The experiments on cell viability were carried out in quadruplicate.

4.5. Lipid peroxidation in mouse brain homogenate

The supernatant fraction of a brain homogenate from male adult C57BL6/J mice (body weight 20–25 g) was prepared as previously described (Hara and Kogure, 1990). Briefly, mice were injected intraperitoneally twice (5-h interval) with either SUN N8075 (30 mg/kg) or vehicle. Brains were removed 1 h after the second injection, then homogenized in a glass-Teflon homogenizer in 4 volumes of ice-cold phosphate saline buffer (50 mM, pH 7.4), and the homogenate was stored at −80 °C. This stock brain homogenate was diluted 10-fold with the same buffer. Then, 1 ml portions of the diluted homogenate were added to 5 μl of the test compound and incubated at 37 °C for 30 min. The reaction was stopped by adding 200 μl of 35% $HClO_4$, followed by centrifugation at 12,000 ×g for 10 min. The supernatant (500 μl) was heated with 250 μl of thiobarbituric acid (TBA) solution (5 g/l in 50% acetic acid) for 15 min at 100 °C. Absorbance was then measured at 532 nm.

4.6. MPTP model in mice

The method used to generate an MPTP model in mice was as previously described (Oida et al., 2006). Mice were injected intraperitoneally with MPTP (10 mg/kg) four times at 1-h intervals, and twice with either SUN N8075 (10 or 30 mg/kg) or vehicle (at 1 h before the first administration of MPTP and 1 h after the last administration of MPTP). Seven days after the MPTP treatment, mice were anesthetized with sodium pentobarbital (nembutal, 50 mg/kg, i.p.) and brains were perfusion-fixed with 4% paraformaldehyde in 0.1 M phosphate-buffer (pH 7.4). The brains were removed after a 20-min perfusion fixation at 4 °C, then immersed in the same fixative solution. Brain sections were dehydrated with graded ethanol, passed through xylene, and embedded in paraffin. Paraffin sections (5 μm thick) of the striatum and substantia nigra were used for immunohistochemistry. The paraffin sections were washed for 5 min in 0.01 M phosphate-buffered saline (PBS), then treated with 0.3% hydrogen peroxidase in 10% methanol. They

were then washed three times in 0.01 M PBS, followed by a 30 min pre-incubation with 10% normal goat serum. They were then incubated either with anti-tyrosine hydroxylase (TH) antibody (1:200), including 0.3% triton X-100, for 3 h at 4 °C or with anti 8-hydroxy-deoxyguanine (8-OHdG) overnight at 4 °C. After a 15-min rinse in changes of 0.01 M PBS, the sections were incubated with biotinylated second antibody for 2 h, and then with an avidin-biotin peroxidase complex for 30 min (both at room temperature). The number of TH-positive neurons in four sections of the substantia nigra from each mouse was counted under the light microscope at a magnification of ×400, and the mean number of TH-positive neurons was calculated. The number of 8-OHdG-positive cells in each section was counted in predefined areas (0.25 mm^2) under the light microscope at a magnification of ×400, and the mean number of 8-OHdG-positive neurons was calculated. Each count of positive cells was performed in a blind manner by a single observer.

4.7. *Statistical analysis*

Data are presented as the means±S.E. Statistical comparisons were made using a one-way ANOVA followed by a Student's t-test or Dunnett's test [using STAT VIEW version 5.0 (SAS Institute, Cary, NC)]. $P<0.05$ was considered to indicate statistical significance.

Acknowledgments

The authors wish to express their gratitude to Mr. Teruyoshi Inoue and Mr. Shigeki Tamura, Biomedical Research Laboratories, Asubio Pharma Co. Ltd, for their helpful discussion.

REFERENCES

Ali, S.F., David, S.N., Newport, G.D., Cadet, J.L., Slikker Jr., W., 1994. MPTP-induced oxidative stress and neurotoxicity are age-dependent: evidence from measures of reactive oxygen species and striatal dopamine levels. Synapse 18, 27–34.

Annoura, H., Nakanishi, K., Toba, T., Takemoto, N., Imajo, S., Miyajima, A., Tamura-Horikawa, Y., Tamura, S., 2000. Discovery of (2S)-1-(4-amino-2,3,5-trimethylphenoxy)-3-[4-[4-(4-fluorobenzyl)phenyl]-1-piperazinyl]-2-propanol dimethanesulfonate (SUN N8075): a dual Na(+) and Ca(2+) channel blocker with antioxidant activity. J. Med. Chem. 43, 3372–3376.

Araki, T., Kumagai, T., Tanaka, K., Matsubara, M., Kato, H., Itoyama, Y., Imai, Y., 2001. Neuroprotective effect of riluzole in MPTP-treated mice. Brain Res. 918, 176–181.

Burns, R.S., Chiueh, C.C., Markey, S.P., Ebert, M.H., Jacobowitz, D.M., Kopin, I.J., 1983. A primate model of parkinsonism: selective destruction of dopaminergic neurons in the pars compacta of the substantia nigra by N-methyl-4-phenyl-1,2,3,6-tetrahydropyridine. Proc. Natl. Acad. Sci. U. S. A. 80, 4546–4550.

Gassen, M., Gross, A., Youdim, M.B., 1998. Apomorphine enantiomers protect cultured pheochromocytoma (PC12) cells from oxidative stress induced by H2O2 and 6-hydroxydopamine. Mov. Disord. 13, 242–248.

Glinka, Y., Gassen, M., Youdim, M.B., 1997. Mechanism of 6-hydroxydopamine neurotoxicity. J. Neural Transm. Suppl. 50, 55–66.

Grims, J.D., Hassan, M.N., Thakar, J.H., 1988. Prevention of progression of Parkinson's disease with antioxidative therapy. Prog. Neuropsychopharmacol. Biol. Psychiatry 12, 165–172.

Hantraye, P., Brouillet, E., Ferrante, R., Palfi, S., Dolan, R., Matthews, R.T., Beal, M.F., 1996. Inhibition of neuronal nitric oxide synthase prevents MPTP-induced Parkinsonism in baboons. Nat. Med. 2, 1017–1021.

Hara, H., Kogure, K., 1990. Prevention of hippocampus neuronal damage in ischemic gerbils by a novel lipid peroxidation inhibitor (quinazoline derivative). J. Pharmacol. Exp. Ther. 255, 906–913.

Hara, H., Ohta, M., Ohta, K., Kuno, S., Adachi, T., 2003. Apomorphine attenuates 6-hydroxydopamine-induced apoptotic cell death in SH-SY5Y cells. Redox Rep. 8, 193–197.

Heikkila, R.E., Manzino, L., Cabbat, F.S., Duvoisin, R.C., 1984. Protection against the dopaminergic neurotoxicity of 1-methyl-4-phenyl-1,2,5,6-tetrahydropyridine by monoamine oxidase inhibitors. Nature 311, 467–469.

Johannessen, J.N., Sobotka, T.J., Weise, V.K., Markey, S.P., 1991. Prolonged alterations in canine striatal dopamine metabolism following subtoxic doses of 1-methyl-4-phenyl-1,2,3,6-tetrahydropyridine (MPTP) and 4ō-amino-MPTP are linked to the persistence of pyridinium metabolites. J. Neurochem. 57, 981–990.

Kasai, H., Nishimura, S., 1986. Hydroxylation of guanine in nucleosides and DNA at the C-8 position by heated glucose and oxygen radical-forming agents. Environ. Health Perspect. 67, 111–116.

Kawasaki, T., Ishihara, K., Ago, Y., Baba, A., Matsuda, T., 2007. Edaravone (3-methyl-1-phenyl-2-pyrazolin-5-one), a radical scavenger, prevents 1-methyl-4-phenyl-1,2,3,6-tetrahydropyridine-induced neurotoxicity in the substantia nigra but not the striatum. J. Pharmacol. Exp. Ther. 322, 274–281.

Kotani, Y., Morimoto, N., Oida, Y., Tamura, Y., Tamura, S., Inoue, T., Shimazawa, M., Yoshimura, S., Iwama, T., Hara, H., 2007. Prevention of *in vitro* and *in vivo* acute ischemic neuronal damage by (2S)-1-(4-amino-2,3,5-trimethylphenoxy)-3-[4-[4-(4-fluorobenzyl) phenyl]-1-piperazinyl]-2-propanol dimethanesulfonate (SUN N8075), a novel neuroprotective agent with antioxidant properties. Neuroscience 149, 779–788.

Nicklas, W.J., Vyas, I., Heikkila, R.E., 1985. Inhibition of NADH-linked oxidation in brain mitochondria by 1-methyl-4-phenyl-pyridine, a metabolite of the neurotoxin, 1-methyl-4-phenyl-1,2,5,6-tetrahydropyridine. Life Sci. 36, 2503–2508.

Oida, Y., Kitaichi, K., Nakayama, H., Ito, Y., Fujimoto, Y., Shimazawa, M., Nagai, H., Hara, H., 2006. Rifampicin attenuates the MPTP-induced neurotoxicity in mouse brain. Brain Res. 1082, 196–204.

Przedborski, S., Ischiropoulos, H., 2005. Reactive oxygen and nitrogen species: weapons of neuronal destruction in models of Parkinson's disease. Antioxid. Redox Signal. 7, 685–693.

Ricaurte, G.A., Langston, J.W., Delanney, L.E., Irwin, I., Peroutka, S.J., Forno, L.S., 1986. Fate of nigrostriatal neurons in young mature mice given 1-methyl-4-phenyl-1,2,3,6-tetrahydropyridine: a neurochemical and morphological reassessment. Brain Res. 376, 117–124.

Robins, P., 2004. Japanese Pharmacological Society—77th Annual Meeting. Part II. 8–10 March 2004, Osaka, Japan. I. Drugs 7, 298–300.

Sankar, S.R., Manivasagam, T., Krishnamurti, A., Ramanathan, M., 2007. The neuroprotective effect of Withania somnifera root extract in MPTP-intoxicated mice: an analysis of behavioral and biochemical variables. Cell. Mol. Biol. Lett. 12, 473–481.

Sato, S., Mizuno, Y., Hattori, N., 2005. Urinary 8-hydroxydeoxyguanosine levels as a biomarker for progression of Parkinson disease. Neurology 64, 1081–1083.

Schneider, J.S., Markham, C.H., 1986. Neurotoxic effects of N-methyl-4-phenyl-1,2,3,6-tetrahydropyridine (MPTP) in the

cat. Tyrosine hydroxylase immunohistochemistry. Brain Res. 373, 258–267.

Soto-Otero, R., Mendez-Alvarez, E., Hermida-Ameijeiras, A., Munoz-Patino, A.M., Labandeira-Garcia, J.L., 2000. Autoxidation and neurotoxicity of 6-hydroxydopamine in the presence of some antioxidants: potential implication in relation to the pathogenesis of Parkinson's disease. J. Neurochem. 74, 1605–1612.

Turski, L., Bressler, K., Rettig, K.J., Loschmann, P.A., Wachtel, H., 1991. Protection of substantia nigra from MPP+ neurotoxicity by *N*-methyl-D-aspartate antagonists. Nature 349, 414–418.

Watanabe, H., Muramatsu, Y., Kurosaki, R., Michimata, M., Matsubara, M., Imai, Y., Araki, T., 2004. Protective effects of neuronal nitric oxide synthase inhibitor in mouse brain against MPTP neurotoxicity: an immunohistological study. Eur. Neuropsychopharmacol. 14, 93–104.

CNS Neuroscience & Therapeutics

Memantine Protects Against Secondary Neuronal Degeneration in Lateral Geniculate Nucleus and Superior Colliculus after Retinal Damage in Mice

Yasushi Ito,[1] Shinsuke Nakamura,[1] Hirotaka Tanaka,[1] Masamitsu Shimazawa,[1] Makoto Araie,[2] and Hideaki Hara[1]

[1] Department of Biofunctional Evaluation, Molecular Pharmacology, Gifu Pharmaceutical University, 5-6-1 Mitahora-Higashi, Gifu 502-8585, Japan
[2] Department of Ophthalmology, University of Tokyo School of Medicine, 7-3-1 Hongo, Bunkyo-ku, Tokyo 113-0033, Japan

Keywords
Glaucoma; Memantine; Mouse; NMDA; Visual pathway.

Correspondence
H. Hara, Department of Biofunctional Evaluation, Molecular Pharmacology, Gifu Pharmaceutical University, 5-6-1 Mitahora-Higashi, Gifu 502-8585, Japan.
Tel.: 81-58-237-8596;
Fax: +81-58-237-8596;
E-mail: hidehara@gifu-pu.ac.jp

doi: 10.1111/j.1755-5949.2008.00050.x

The purpose of this study, on mice, was to determine whether memantine, a glutamate-receptor antagonist of the *N*-methyl-D-aspartate (NMDA) subtype, protects against neuronal degeneration in the dorsal lateral geniculate nucleus (dLGN) and superior colliculus (SC) after the induction of retinal damage by intravitreal injection of NMDA.

NMDA (20 mM/2 μl) was injected into the vitreous body of the left eye in mice (day 0). To evaluate the neuroprotective effect of memantine, mice were assigned to one of two memantine-treated groups: receiving a daily administration of memantine at 30 mg/kg/day, p.o. either from day 0 (administered at 1 h before NMDA injection) to day 90 (pretreated group) or from day 7 to day 90 (post-treated group).

The pretreated group exhibited significant suppression of the retinal damage induced by intravitreal injection of NMDA and significant prevention of transsynaptic neuronal degeneration in the dLGN and SC on the contralateral side. Although the mice of the post-treated group displayed no reversion of such retinal damage, they did exhibit protection against neuronal degeneration in the LGN and SC on the contralateral side. These data indicate that memantine can protect against transsynaptic neuronal degeneration in the murine brain (LGN and SC) even if treatment is begun after retinal ganglion cell (RGC) death has started.

Memantine protects against the secondary neuronal degeneration in brain regions in the visual pathway that occurs after retinal damage in mice.

Introduction

Memantine, 1-amino-3,5-dimethyladamantane, an *N*-methyl-D-aspartate (NMDA) antagonist, has therapeutic potential against several central nervous system (CNS) disorders [1]. In the United States and Europe, memantine has been used clinically for moderate to severe Alzheimer's disease [2] for a number of years. In addition, it has been reported that memantine shows evidence of therapeutic benefits in several animal models of glaucoma, the leading cause of blindness [3–5]. In glaucoma, the concentration of glutamate, the principal excitatory neurotransmitter, has been reported to be increased in the vitreous body [6], although this finding was not confirmed by [7]. Be that as it may, it is known that the toxic effects of elevated glutamate levels are predominantly mediated by overstimulation of ionotropic receptors. Overstimulation of the class of these receptors that respond specifically to the glutamate analog NMDA has been shown to contribute to the death of retinal ganglion cells (RGC) [8,9].

The animal model employed in the present study (involving intravitreal injection of NMDA) shows decreasing cell number in the ganglion cell layer (GCL) [10].

Because of its high sensitivity, stability, and good reproducibility, this model has been widely used for investigating the mechanisms underlying neuronal cell death in the retina [11]. Our previous study on this model revealed that dramatic retinal damage occurred within 7 days after NMDA injection, and that subsequently neurons in the lateral geniculate nucleus (LGN), the major relay center between the eye and the visual cortex, were decreased in number at 90 days after the NMDA injection [12–14]. There is also recent evidence that the RGC death that occurs in glaucoma models leads to neuronal degeneration within the LGN [15,16]. Furthermore, while a loss of more than 50% of RGC has been reported to induce visual field loss, the initial loss of RGC in glaucoma patients does not lead to visual field loss [17]. These data suggest that the visual field loss induced by glaucoma may result not only from RGC loss, but also from neuronal degeneration within LGN [18].

Although it is generally believed that in rodents most axonal projections from the retina pass to SC, with only a small percentage of axons going to LGN, visual information entering the human eye is processed in the retina and transmitted via the optic nerve to LGN. This suggests that protection of neurons within LGN, as well as retinal treatment, could be effective for the prevention of eye diseases that cause blindness, such as glaucoma. Therefore, in this study we investigated these two pathways (retino-geniculate and retino-superior colliculus pathways) in mice. With the aim of determining whether memantine might protect against the secondary neuronal degeneration within the visual pathway (LGN and SC) that occurs after RGC damage.

Materials and Methods

All experiments were performed in accordance with the ARVO Statement for the Use of Animals in Ophthalmic and Vision Research, and they were approved and monitored by the Institutional Animal Care and Use Committee of Gifu Pharmaceutical University.

Animal Subjects

Male adult C57BL/6J mice weighing 20–32 g (Clea Japan Inc., Fujimiya, Japan) were kept under lighting conditions of 12 h light and 12 h dark. They were anesthetized with 3.0% isoflurane (Merck, Osaka, Japan) and maintained with 1.5% isoflurane in 70% N_2O and 30% O_2 via an animal general anesthesia apparatus (Soft Lander; Sin-ei Industry Co. Ltd., Saitama, Japan). Retinal damage was induced (on day 0) by the intravitreal injection (2 μl/eye) of NMDA (Sigma-Aldrich, St. Louis, MO) dissolved at 20 mM in 0.01 M phosphate-buffered saline (PBS) at pH 7.4. This was injected into the vitreous body of the left eye under the above anesthesia. One drop of levofloxacin ophthalmic solution (Santen Pharmaceuticals Co. Ltd., Osaka, Japan) was applied topically to the treated eye immediately after the intravitreal injection. Mice that received intravitreal NMDA were also treated either with memantine (30 mg/kg, p.o.) (Merz Pharmaceuticals GmbH., Frankfurt, Germany) or with the vehicle for memantine (distilled water, p.o.) by oral gavage for the periods detailed below (memantine or vehicle administration was started at 1 h before NMDA injection). For simplicity the latter (NMDA + vehicle-treated) group is referred to hereafter as the "vehicle-treated group." Mice receiving an intravitreal injection of saline instead of NMDA were prepared for sham-treated group. Mice were euthanized either on day 7 (Fig. 3) or on day 90 (Figs. 4–8). For most experiments (i.e., those illustrated by Figs. 4–8), four groups of mice were evaluated and compared: (i) sham-treated group, (ii) vehicle-treated group [mice receiving an intravitreal injection of NMDA and also (from day 0 to day 90; p.o.) the vehicle for memantine], (iii) pretreated group (mice receiving an intravitreal injection of NMDA and also a daily administration of memantine at 30 mg/kg, p.o. from day 0 to day 90), and (iv) post-treated group (mice receiving an intravitreal injection of NMDA and also a daily administration of memantine at 30 mg/kg, p.o. from day 7 to day 90) (Fig. 1).

For the experiment illustrated by Figure 3, only three groups of mice were employed: (i) sham-treated group (mice receiving an intravitreal injection of saline instead of NMDA), (ii) vehicle-treated group [mice receiving an intravitreal injection of NMDA and also (from day 0 to day 7; p.o.) the vehicle for memantine], (iii) memantine-treated group (mice receiving an intravitreal injection of NMDA and also a daily administration of memantine at 30 mg/kg, p.o. from day 0 to day 7).

Tissue Processing

At the end of their assigned survival period, mice were anesthetized with sodium pentobarbital (80 mg/kg, i.p.) (Nembutal; Dainippon, Osaka, Japan), then perfused with 2% (w/v) paraformaldehyde solution in 0.01 M PBS. The brains were removed after 15 min perfusion at 4°C, immersed in the same fixative solution for 24 h, soaked in 25% (w/v) sucrose for 1 day, then frozen in embedding compound (Tissue-Tek; Sakura Finetechnical Co. Ltd., Tokyo, Japan). Serial coronal sections through the levels of the LGN (bregma −2.10 ~ −2.40 mm) and superior colliculus (SC) (bregma −3.20 ~ −3.50 mm) were cut at 50-μm thickness, then stained with cresyl violet. Each eye was enucleated at the time of brain

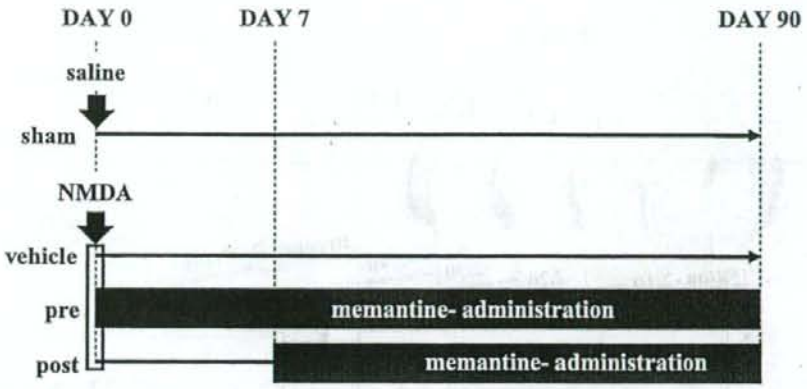

Figure 1. Schedule for memantine administration in the experiments illustrated by Figs. 4–8. Mice were euthanized at 90 days after NMDA intravitreous injection. Four groups of mice were evaluated and compared: (i) sham-treated group (mice received an intravitreal injection of saline instead of NMDA), (ii) vehicle-treated group (mice receiving an intravitreal injection of NMDA and also a daily oral administration of the vehicle for memantine from day 0 to day 90), (iii) pretreated group (mice intravitreally injected with NMDA who also received a daily administration of memantine at 30 mg/kg, p.o. from day 0 to day 90), and (iv) post-treated group (mice intravitreally injected with NMDA who also received a daily administration of memantine at 30 mg/kg, p.o. from day 7 to day 90).

removal, and 4% paraformaldehyde solution was injected into the vitreous body. The eye was then kept immersed for at least 24 h in the same fixative solution at 4°C. Six paraffin-embedded sections (thickness, 5 μm) cut through the optic disc of each eye were prepared in a standard manner, then stained with hematoxylin and eosin.

Histological Analysis of Mouse Retina

Retinal damage was evaluated as previously described [11], three of the six sections stained with hematoxylin and eosin from each eye being used for the morphometric analysis. Light-microscope photographs were taken using a digital camera (Coolpix 4500, Nikon) and the cell counts in the GCL and the thickness of the inner plexiform layer (IPL) at a distance between 375 and 625 μm from the optic disc were measured on the images in a masked fashion by a single observer (S.N.). Data from three sections (selected randomly from the six sections) were averaged for each eye, and the values obtained were used to evaluate the GCL cell count and the IPL thickness.

Neuron Numbers in dLGN and SC

To assess the protective effects of memantine against neuronal loss in dorsal lateral geniculate nucleus (dLGN) and SC, sections stained with cresyl violet were used for neuronal cell counting: four sections for dLGN (L1: bregma −2.10 mm, L2: −2.20 mm, L3: −2.30 mm, and L4: −2.40 mm) and four for SC (S1: bregma −3.20 mm, S2: −3.30 mm, S3: −3.40 mm, and S4: −3.50 mm), respectively, in each mouse (Fig. 2A). The area of each field used for this cell counting was 0.047 mm^2 of dLGN (Fig. 2B and D) and 0.047 mm^2 of the superficial layer of SC (Fig. 2C and E). Cell counts were carried out under a microscope at 400× magnification in a masked fashion by a single observer (S.N.). Care was taken to count only neurons with clearly visible nuclei and cytoplasm.

Volume of dLGN

Measurements of the surface area of dLGN were made in four equally spaced sections (interval, 100 μm) from section L1 to section L4 (i.e., the sections counting the bulk of dLGN). These area measurements were carried out under a microscope at 100× magnification in a masked fashion by a single observer (S.N.), recorded as images using a digital camera (Nikon Coolpix 4500), and then quantitated using Image J. Cavalieri's estimator of volume was used to calculate the volume (V_T) of dLGN (bregma −1.70 ~ −2.90 mm) using the following formula:

$$V_T = \Sigma a_i \times s_t$$

where a_i is the cross-sectional area of the dLGN in the ith profile and s_t is the mean distance between sections

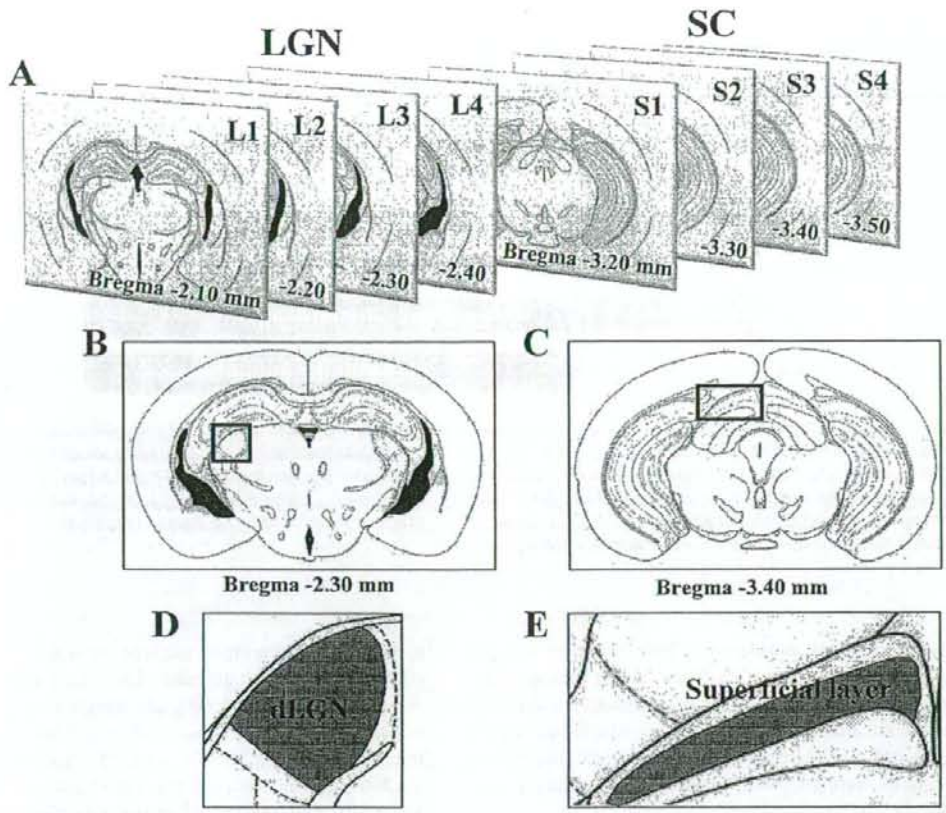

Figure 2. Illustrations showing (A) serial coronal sections through levels of LGN (bregma −2.10 ~ −2.40 mm) and SC (bregma −3.20 ~ −3.50 mm) in mice. Coronal sections through levels of LGN (bregma −2.30 mm) (B) and SC (bregma −3.40 mm) (C) in mice (boxed areas are shown diagrammatically in (D) and (E), respectively).

(section thickness multiplied by the inverse of the periodicity of sections in the series) [19].

Statistical Analysis

Data are presented as means ± S.E.M. Statistical comparisons (one-way ANOVA followed by a Student's *t*-test) were made using STAT VIEW version 5.0 (SAS Institute, Inc., Cary, NC, USA). A value of $P < 0.05$ was considered to indicate statistical significance.

Results

Protective Effect of Memantine Against Retinal Damage at 7 Days after NMDA Injection

Intravitreal injection of NMDA at 40 nmol/eye decreased both the cell count in GCL (32.7 ± 3.1 cells/mm, n = 8) and the thickness of IPL (13.2 ± 0.9 μm, n = 8) in the retina (Fig. 3B, D, and E) versus those in the sham-treated retina (135.0 ± 9.2 cells/mm for GCL and 36.8 ± 2.3 μm for IPL, n = 8; $P < 0.05$ in each case) (Fig. 3A, D, and E). The memantine-treated group (mice receiving an intravitreal injection of NMDA who also received a daily administration of memantine at 30 mg/kg, p.o. from day 0 to day 7) displayed significant suppression of both of these decreases (54.5 ± 6.3 cells/mm for GCL and 19.8 ± 1.2 μm for IPL, n = 8) (Fig. 3C, D, and E).

Protective Effect of Memantine Against Retinal Damage at 90 Days after NMDA Injection

The pretreated group displayed a significantly greater cell number in GCL (37.7 ± 2.3 cells/mm, n = 8) than the vehicle-treated group (28.1 ± 1.2 cells/mm, n = 7)

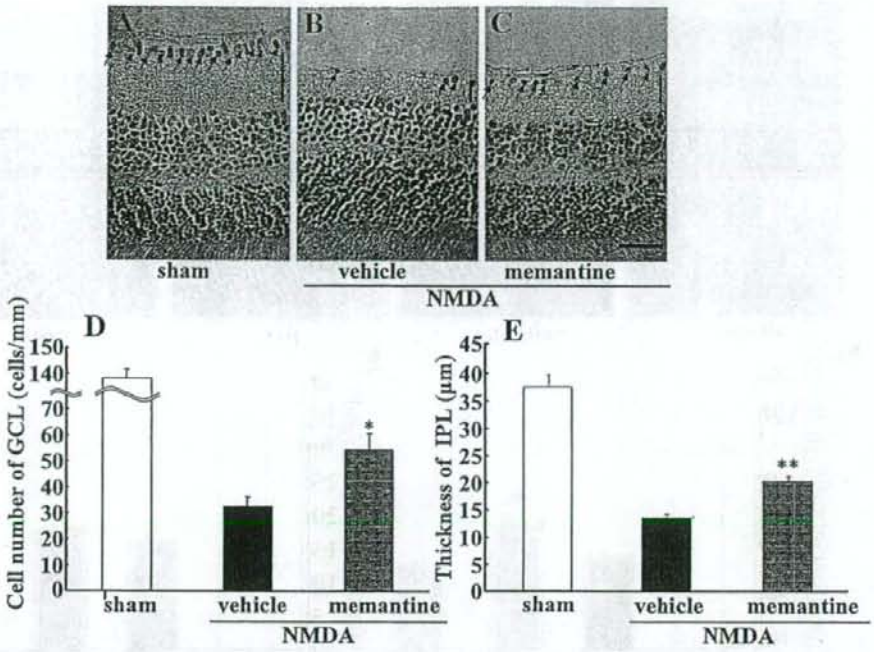

Figure 3. Protective effect of memantine against retinal damage, as assessed at 7 days after NMDA intravitreous injection. Representative photographs of retinas from sham-treated (**A**), vehicle-treated (**B**), and memantine (30 mg/kg/day p.o.)-treated (**C**) groups. Vertical bars show thickness of IPL. Horizontal bar represents 20 μm. Arrows indicate live cells within GCL. Cells number in GCL (**D**) and thickness of IPL (**E**) were measured. Each value represents the mean ± S.E.M. for 8 eyes. $^{*}P < 0.05$, $^{**}P < 0.01$ versus vehicle (Student's *t*-test).

(Fig. 4B, C, and E). On the other hand, in the thickness of IPL there was no significant difference between the vehicle-treated group (17.1 ± 0.9 μm, n = 7) and the pretreated group (18.5 ± 0.7 μm, n = 12), although the latter group tended to show a suppressed decrease in IPL thickness versus the vehicle-treated group (Fig. 4B, C, and F). The post-treated group showed no significant difference from the vehicle-treated group in either of the NMDA-induced decreases (25.3 ± 1.7 cells/mm for GCL and 14.7 ± 0.4 μm for IPL, n = 12) (Fig. 4B, D–F).

Neuron Numbers in dLGN

In the contralateral dLGN, the numbers of neurons in the vehicle-treated group were 60.5 ± 2.5 (n = 8), 61.5 ± 3.0 (n = 8), 62.8. ± 4.8 (n = 8), and 65.5 ± 1.7 (n = 8) in sections L1, L2, L3, and L4, respectively. Each of these counts was smaller than the corresponding one for contralateral dLGN neurons in the sham-treated group (94.3 ± 3.4, 98.9 ± 5.0, 103.0 ± 3.5, and 93.1 ± 3.9, respectively, each n = 8; $P < 0.05$ in each case) (Fig. 5A, B, and E). The pretreated group (78.8 ± 4.3 for L1, 80.6 ± 4.0 for L2, 83.3 ± 4.4 for L3, and 74.5 ± 1.8 for L4, each n = 8) and the post-treated group (70.6 ± 2.9 for L1, 76.3 ± 3.8 for L2, and 78.1 ± 3.7 for L3, each n = 8) exhibited significantly greater contralateral dLGN neuron numbers than the vehicle-treated group (Fig. 5B–E). In contrast, in the ipsilateral dLGN there were no significant differences in numbers of neurons among the four groups (sham-, vehicle-, pre-, and post-treated mice) (Fig. 5F).

Volume of dLGN

The volume of the contralateral dLGN was smaller in the vehicle-treated group (0.124 ± 0.003 mm^3, n = 6) than in the sham-treated group (0.153 ± 0.007 mm^3, n = 6; $P < 0.05$) (Fig. 6A, B, and E). The pretreated group (0.137 ± 0.002 mm^3, n = 6) and the post-treated group (0.136 ± 0.002 mm^3, n = 8) exhibited significantly greater contralateral dLGN volumes than the vehicle-treated group (Fig. 6B–E). In contrast, in the ipsilateral

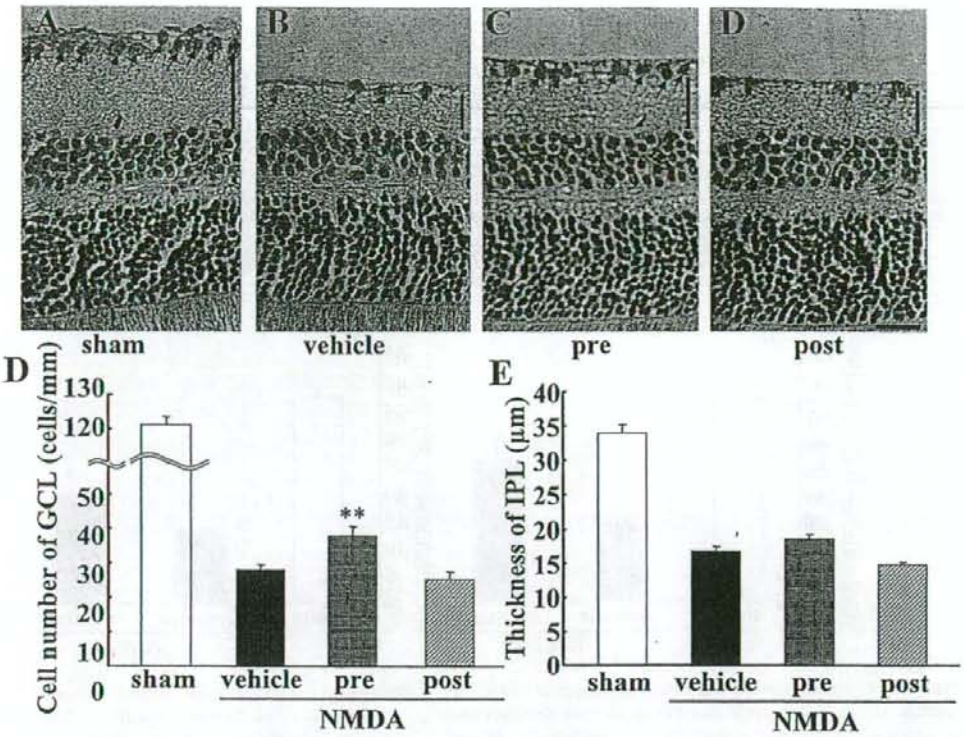

Figure 4. Protective effect of memantine against retinal damage (assessed on day 90). Representative photographs of retinas from sham-treated (**A**), vehicle-treated (**B**), pretreated (**C**), and post-treated (**D**) groups. Vertical bars show thickness of IPL. Horizontal bar represents 20 μm. Arrows indicate live cells within GCL. Cells number in GCL (**E**) and thickness of IPL (**F**) were measured. Each value represents the mean ± S.E.M. for 7–12 eyes. $^{**}P < 0.01$ versus vehicle (Student's *t*-test).

dLGN there were no significant differences in volume among the four groups (sham-, vehicle-, pre-, and post-treated mice) (Fig. 6E).

Neuron Numbers in SC

In the contralateral SC, the numbers of neurons in the vehicle-treated group were 48.8 ± 1.8 (n = 8), 50.1 ± 2.9 (n = 8), 51.8 ± 2.7 (n = 8), and 50.4 ± 3.2 (n = 8) in sections S1, S2, S3, and S4, respectively. Each of these counts was smaller than the corresponding one for contralateral SC neurons in the sham-treated group (85.3 ± 2.3, 85.4 ± 2.5, 82.5 ± 3.7, and 84.6 ± 1.5, respectively, each n = 8; $P < 0.05$ in each case) (Fig. 7A, B, and E). The pretreated group (64.9 ± 2.4 for S1, 63.5 ± 2.7 for S2, 63.4 ± 3.5 for S3, and 64.6 ± 4.3 for S4, each n = 8) and the post-treated group (63.6 ± 1.8 for S1, 61.8 ± 3.1 for S2, 60.1 ± 2.7 for S3, and 63.9 ± 4.2 for S4, each n = 8) exhibited significantly greater contralateral SC neuron numbers than the vehicle-treated group (Fig. 7B–E). In contrast, in the ipsilateral SC there were no significant differences in the numbers of neurons among the four groups (sham-, vehicle-, pre-, and post-treated mice) (Fig. 7F).

Discussion

The purpose of this study was to determine whether memantine exerts protective effects against secondary neuronal degeneration in the dLGN and SC following retinal damage in mice. In this study, we introduce the first murine model for evaluation of the effects of drugs on the changes in brain areas that occur following intravitreal injection of NMDA.

First, we had to choose an appropriate concentration of memantine for the evaluation of its neuroprotective

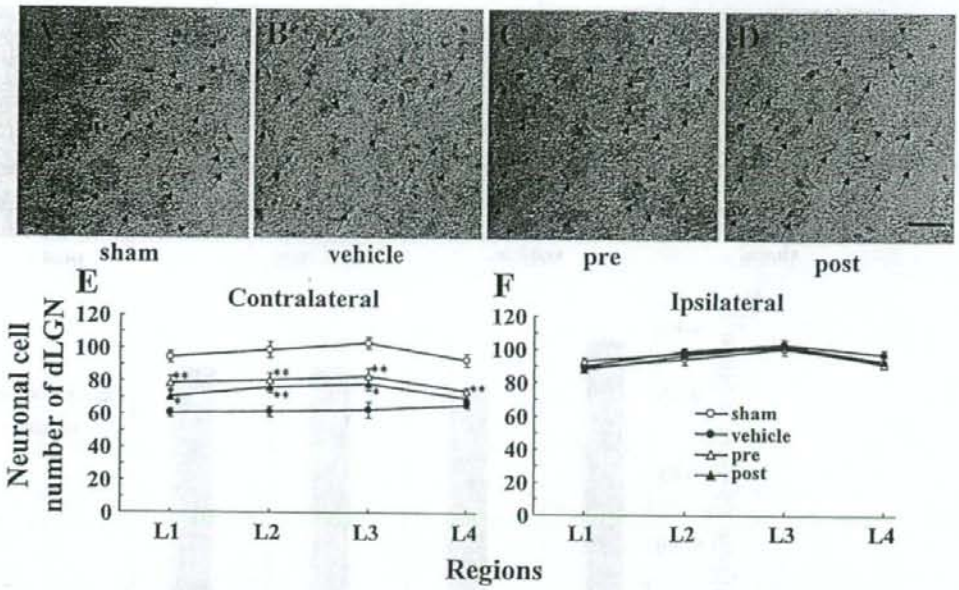

Figure 5. Protective effect of memantine against neuronal loss in dLGN (assessed on day 90). Representative photographs from sham-treated group (**A**), vehicle-treated group (**B**), pretreated group (**C**), and post-treated group (**D**). Neuronal cell number within dLGN was measured on the contralateral (**E**) and ipsilateral (**F**) sides. Coronal sections through level of dLGN (L1: bregma −2.10 mm, L2: −2.20 mm, L3: −2.30 mm, and L4: −2.40 mm). In each field, the tissue area of dLGN examined was 0.047 mm^2. Horizontal bar represents 20 μm. Arrows (in **A–D**) indicate neuronal cells. Each value represents the mean ± S.E.M. for eight brains. $^*P < 0.05$, $^{**}P < 0.01$ versus vehicle (Student's *t*-test).

effects within the murine brain. Previous preclinical and clinical studies have indicated that the therapeutic plasma concentration of memantine is between 0.5 and 1 μM [20, 21]. Therefore, to mimic clinically relevant conditions an oral dose of 30 mg/kg was selected on the basis of a pilot study that showed that this produced a steady-state plasma level of 1.14 μM in C57BL/6J mice [22].

In this study, we found that mice receiving memantine from day 0 displayed significantly attenuated retinal damage at both 7 and 90 days after an intravitreal injection of NMDA (Figs. 3 and 4). An effect of memantine has been demonstrated on similar the retinal injury induced by glutamate toxicity in rats [23]. Memantine has previously been shown to suppress spontaneous RGC degeneration in a normal tension glaucoma model involving mice deficient in the glutamate/aspartate transporter (GLAST) [24]. Taken together, these data suggest that systemic administration of memantine may act on NMDA receptors located in the retina and thereby protect RGC from glutamate excitotoxicity [25]. On the other hand, our post-treated group did not show reversion of NMDA-induced retinal damage (Fig. 4). Since dramatic retinal damage has occurred by day 7 in the present model [10, 14; present study], daily administration of memantine from day 7 may be too late to rescue RGC to a significant degree through a blockage of excessive glutamate-receptor activation.

Next, we examined the neuroprotective effects of memantine within the LGN and SC after retinal damage. Neuronal loss was evident in the contralateral dLGN (number of neurons and volume) and in the contralateral SC (number of neurons) on day 90 after intravitreal NMDA injection (Figs. 5–7). Such neuronal loss may result from a reduction in the visual stimuli transmitted from RGCs and from a depletion of neurotrophins associated with a dysfunction of anterograde transport from RGCs [26]. These affects may lead to "Wallerian degeneration," a process in which the part of the axon separated from the neuron's cell nucleus will degenerate [27]. In this study, our findings indicate that in addition to the pretreated group, the post-treated group also exhibited evidence of protective effects of memantine against neuronal degeneration in the brain (LGN and SC), although the latter group displayed no significant difference in GCL cell number versus the vehicle-treated group (Figs. 4–8). These findings suggest that memantine protected against

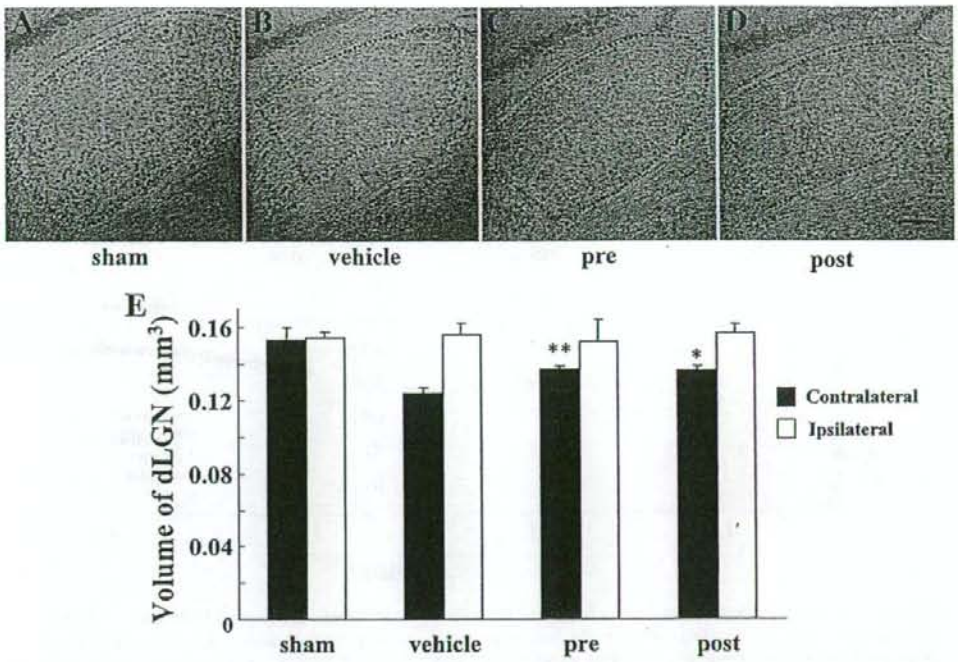

Figure 6. Protective effect of memantine against shrinkage of dLGN volume (assessed on day 90). Representative photographs from sham-treated group (**A**), vehicle-treated group (**B**), pretreated group (**C**), and post-treated group (**D**). The contralateral and ipsilateral dLGN volumes were measured (**E**). Horizontal bar represents 100 μm. Each value represents the mean ± S.E.M. for six to eight brains. $^{*}P < 0.05$, $^{**}P < 0.01$ versus vehicle (Student's *t*-test).

secondary neuronal degeneration within the LGN and SC after retinal damage. Such cerebroprotection after retinal damage may allow retention of a compensatory action within the brain that serves to prevent visual field loss after retinal damage. Possibly, the neuroprotective mechanisms by which memantine acts within the brain may involve it acting on the NMDA-receptor subtype expressed by the relay neurons within the LGN [28, 29], and it may rescue neurons by blocking the excessive glutamate-receptor activation that contributes to the pathobiology of glaucomatous neural degeneration [8]. In fact, in an experimental ocular hypertension model involving glaucomatous monkeys, memantine has been found to be effective against optic nerve-fiber loss and neuron-shrinkage within the LGN by preventing the transsynaptic degeneration involved in glutamate excitotoxicity [3,5].

In addition, in a mechanism distinct from NMDA-receptor antagonism, memantine specifically upregulate the mRNA and protein expressions of brain-derived neurotrophic factor (BDNF) and its specific tropomyosin receptor kinase B (Trk B), which are implicated in cell survival [30, 31]. Thus, the neuroprotective effects of memantine may be related to enhanced expressions of endogenous growth factors within the LGN [32]. In fact, Trk B is expressed in LGN neurons [33] and it protects cortical neurons through the extracellular signal-regulated kinase (ERK) and phosphatidylinositol 3-kinase (PI3K) pathways [34, 35]. Memantine may enhance these cell-survival signals, and this may be the mechanism by which it protected neuronal cells in the LGN and SC in the present study.

Using mice is easy to long-term administration of memantine and further studies using transgenic mice may be an effective way of elucidating the mechanisms underlying neuronal degeneration and protection in brain after retinal damage. Therefore, mice were used in the present study. Since the protective mechanism by which memantine acts in the murine LGN and SC was not determined in this study, further studies will be needed to clarify the precise mechanism. In the meantime, we propose that in addition to therapies aimed at rescuing RGCs directly, a neuroprotective strategy aimed at rescuing neurons within the brain (LGN and SC) after RGC damage

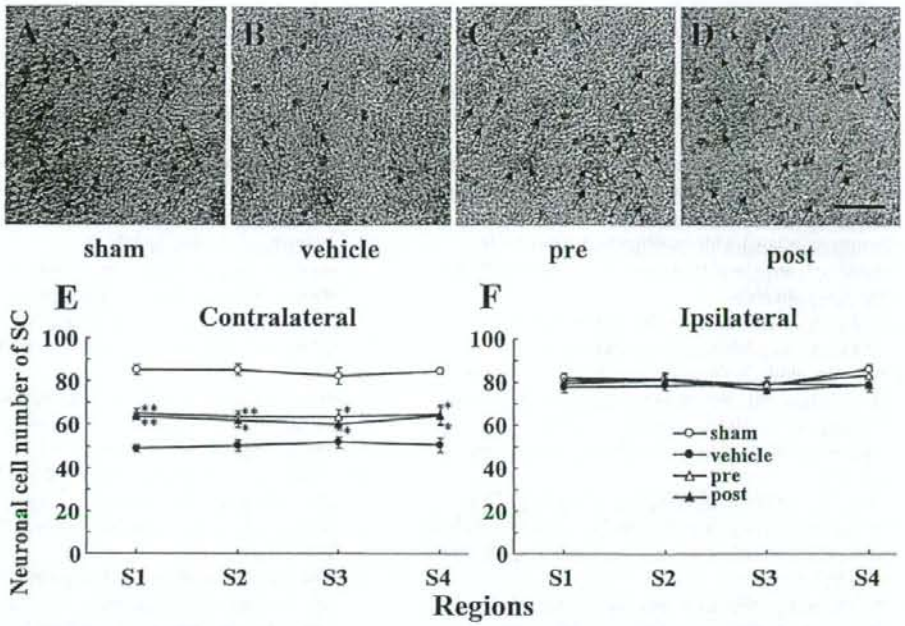

Figure 7. Protective effect of memantine against neuronal loss within SC (assessed on day 90). Representative photographs from sham-treated group (**A**), vehicle-treated group (**B**), pretreated group (**C**), and post-treated group (**D**). Neuronal cell number within SC was measured on the contralateral (**E**) and ipsilateral (**F**) sides. Coronal sections through level of SC (S1: bregma −3.20 mm, S2: −3.30 mm, S3: −3.40 mm, and S4: −3.50 mm). In each field, the tissue area of SC examined was 0.047 mm^2. Horizontal bar represents 20 μm. Arrows (in A–D) indicate neuronal cells. Each value represents the mean ± S.E.M. for eight brains. $^{**}P < 0.01$ versus vehicle (Student's *t*-test).

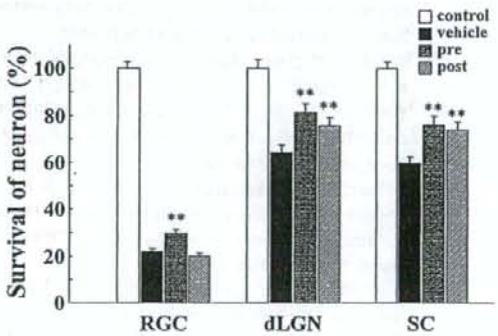

Figure 8. Summary of derived from data shown in Figs. 4, 5, and 7. For RGC, dLGN, and SC, neuron survival in vehicle-treated, pre-treated, and post-treated groups was compared with that in the sham-treated (control) group. Data from four sections (L1–L4 and S1–S4, respectively) were averaged for each brain, and these were used to evaluate survival neurons within the LGN and SC. $^{**}P < 0.01$ versus vehicle (Student's *t*-test).

may be of therapeutic benefit in preventing or reducing visual field loss, possibly by permitting a compensatory action to remain in operation within the brain.

Acknowledgments

The authors wish to express their gratitude Merz Pharmaceuticals GmbH., Frankfurt, Germany for kind gift of memantine and support in part by grants-in-aid for exploratory research from the Ministry of Education, Culture, Sports, Science, and Technology, Japan (Nos. 18209053 and 18210101) and grant-in-aid from the Japan Society for the Promotion of Science (No. 20-10786).

Conflict of Interest

The authors have no conflict of interest.

References

1. Parsons CG, Danysz W, Quack G. Memantine is a clinically well tolerated *N*-methyl-D-aspartate (NMDA)